Superconductivity-induced dynamic and static changes in $\mathbf{q}\neq\mathbf{0}$ phonons of high-T_c oxides

R. Zeyher
Max-Planck-Institut für Festkörperforschung, D-7000 Stuttgart 80, Federal Republic of Germany
(Received 8 April 1991)

Superconductivity-induced self-energies of $\mathbf{q}\neq\mathbf{0}$ phonons and changes in static local lattice properties are calculated for $YBa_2Cu_3O_7$ using strong-coupling theory, the harmonic approximation for phonons in the normal state, and a recently introduced screened ionic model for the electron-phonon coupling. The main results are (i) dynamic changes in the frequency and the damping of phonons decrease with increasing momentum, however, they still should be observable for momentum transfers up to $|\mathbf{q}|\sim 2k_F$ and phonon frequencies near the gap and (ii) in spite of the low Fermi energy and a rather large average coupling constant λ of about 3, relative changes due to superconductivity in static quantities such as the Debye-Waller factor and the kinetic energy of an atom are very small and of the order of 10^{-3}. Recently reported large changes in channeling rates and in the width of a Cu nuclear-absorption resonance near and below T_c thus remain unexplained within the present approach.

I. INTRODUCTION

Our present theoretical understanding of the normal and superconducting properties of high-T_c superconductors is rather poor. The application of conventional concepts or new ideas has so far not led to a generally accepted basis for the interpretation of the experimental data. Even the basic question of whether the electron-phonon coupling is small or large in high-T_c oxides could not be settled. Based on the small observed isotope effects,[1] the behavior of the resistivity[2] (linear temperature dependence, absence of saturation effects), and band-structure calculations,[3–6] it has been widely concluded that the electron-phonon coupling is small in high-T_c oxides and irrelevant for superconductivity.

A rather direct way to probe the interaction of phonons with electrons near the Fermi surface consists in studying superconductivity-induced changes in lattice properties. By measuring the temperature dependence of lattice properties, it is often possible to separate a superconducting-related part from the background due to its pronounced temperature dependence near or below T_c. Theoretically, such changes can also be calculated without having to specify many nonuniversal quantities because only properties near the Fermi surface enter. Superconductivity-induced softenings, hardenings, and dampings have been observed for several $\mathbf{q}=\mathbf{0}$ phonons in $YBa_2Cu_3O_7$ (Refs. 7–10) and can be explained quantitatively within a strong-coupling approach.[11,12] Local-density-approximation (LDA) calculations of $\mathbf{q}=0$ phonons, which contain long-range contributions but not possible enhancement effects due to Coulomb correlations, yield a dimensionless electron-phonon-coupling constant of $\lambda\sim 0.5-2$.[13,14] The observed rise and maximum in the heat conductivity in $YBa_2Cu_3O_7$ below T_c (Refs. 15 and 16) has been explained within a conventional approach with an average coupling constant of $\lambda_{br}\sim 0.4-0.5$ for the longitudinal acoustic branch.[17] Since there are 39 branches and since all branches should contribute, one expects that the total electron-phonon-coupling constant λ is one order of magnitude larger than individual branch-coupling constants. The above observations therefore suggest the presence of a strong electron-phonon coupling in $YBa_2Cu_3O_7$.

It is desirable to extend the above results for $\mathbf{q}=0$ and acoustic phonons to a general phonon branch and a general point in the Brillouin zone. Experimentally, inelastic neutron scattering as function of temperature would be an ideal tool for such investigations. A possible observation of superconductivity-induced changes for a general phonon would depend on the momentum dependence of the electron-phonon coupling, on the momentum dependence of the change of the polarization function $\delta\Pi$ due to superconductivity, and on the phonon frequency relative to the gap. The screened ionic model of Ref. 18 suggests that the electron-phonon coupling does not decrease with momentum on the average. On the other hand, one expects intuitively that $\delta\Pi$ decreases substantially with increasing momentum transfer, especially for values larger than the diameter of the Fermi surface. Similarly, $\delta\Pi$ should decrease for frequencies far away from the gap, so that only phonons near the gap are influenced by superconductivity. In order to quantify these expectations, we present in Sec. II calculations for the frequency and momentum dependence of $\delta\Pi$ for a one-band model with cylindrical symmetry; this describes approximately the conduction band of a CuO_2-layer. We also give in this section a more fundamental derivation of the change in the self-energy of a phonon due to superconductivity than in Refs. 11 and 12. Such a more general derivation is needed to be able to include Fermi-liquid corrections. The present approach thus contributes also to the question of whether strong electronic correlations increase or decrease electron-phonon effects.

The results of Sec. II are used in Sec. III to calculate the superconductivity-induced change in the kinetic energy and Debye-Waller factor of a copper and an oxygen atom in the plane. One basic assumption is that the pho-

nons of the normal state can be described within the harmonic approximation by a phenomenological model.[19] It is shown analytically for $\mathbf{q}=0$ and the BCS case that only very small effects due to superconductivity are left once the sum over Matsubara frequencies is carried out. Numerical calculations, both for strong and weak coupling, confirm this conclusion. Finally, we compare our results with recent experiments.

II. SUPERCONDUCTIVITY-INDUCED SELF-ENERGY OF $\mathbf{q}\neq 0$ PHONONS

The electronic contribution to the frequency-dependent dynamical matrix is given by[20]

$$\Phi_{\alpha\beta}\begin{bmatrix} l & l' \\ \kappa & \kappa' , i\omega_n \end{bmatrix} = \int d\mathbf{r}\, d\mathbf{r}' \frac{\partial V(\mathbf{r})}{\partial x_\alpha \begin{bmatrix} l \\ \kappa \end{bmatrix}} \chi(\mathbf{r}\mathbf{r}', i\omega_n) \frac{\partial V(\mathbf{r}')}{\partial x_\beta \begin{bmatrix} l' \\ \kappa' \end{bmatrix}} + \text{ self-terms.} \tag{1}$$

$x_\alpha\binom{l}{\kappa}$ denotes the αth Cartesian component of the position vector of an ion with cell and basis indices l and κ, respectively. ω_n stands for the bosonic Matsubara frequency $2\pi nT$ with n and T being an integer and the temperature, respectively. V denotes the bare electron-core interaction. The self-terms, not written out in Eq. (1), are diagonal in l and κ and can be determined from the first term on the right-hand side of Eq. (1) from the requirement of translational invariance. χ is the dynamical susceptibility which obeys the equation[21]

$$\chi(\mathbf{r}\mathbf{r}', i\omega_n) = \Pi(\mathbf{r}\mathbf{r}', i\omega_n) + \int d\mathbf{r}''\, d\mathbf{r}'''\, \Pi(\mathbf{r}\mathbf{r}'', i\omega_n) v(\mathbf{r}''-\mathbf{r}''') \chi(\mathbf{r}'''\mathbf{r}', i\omega_n) \ . \tag{2}$$

v is the Coulomb interactions, and Π is the irreducible susceptibility whose diagrams cannot be disconnected by cutting one Coulomb line. Using Nambu's 2×2 matrix notation, the general expression for Π has the form[21]

$$\Pi(\mathbf{r}\mathbf{r}', i\omega_n) = T\sum_{n'} \mathrm{Tr} \int d\mathbf{r}''\, d\mathbf{r}'''\, \tau_3 G(\mathbf{r}\mathbf{r}'', i\epsilon_{n'} + i\omega_n) \Gamma'(\mathbf{r}''\mathbf{r}''', i\epsilon_{n'} + i\omega_n, i\epsilon_{n'}) G(\mathbf{r}'''\mathbf{r}', i\epsilon_{n'}) \ . \tag{3}$$

Tr denotes the trace over the two Nambu matrix indices. G is the 2×2 one-particle Green's function, and ϵ_n are the fermionic Matsubara frequencies $(2n-1)\pi T$. Neglecting higher-order phonon interactions, Γ' denotes an irreducible Coulomb vertex which is related to the self-energy of G in the limit $\omega_n, \mathbf{k}\to 0$, by a Ward identity.

In the following we are interested in the changes $\delta\Phi$ of the dynamical matrix caused by superconductivity. From Eq. (2) it follows that changes in χ are related to those in Π by

$$\delta\chi = (1-\Pi v)^{-1} \delta\Pi (1-v\Pi)^{-1} \ , \tag{4}$$

omitting the arguments $\mathbf{r}\mathbf{r}', i\omega_n$ and using a matrix notation. Defining the dielectric matrix ϵ by

$$\epsilon = 1 - v\Pi \tag{5}$$

and omitting the self-terms in Eq. (1), we obtain

$$\delta\Phi_{\alpha\beta}\begin{bmatrix} l & l' \\ \kappa & \kappa' , i\omega_n \end{bmatrix} = \int d\mathbf{r}\, d\mathbf{r}'\, g^*_\alpha \begin{bmatrix} l \\ \kappa , \mathbf{r}, i\omega_n \end{bmatrix} \delta\Pi(\mathbf{r}\mathbf{r}', i\omega_n) g_\beta \begin{bmatrix} l' \\ \kappa' , \mathbf{r}', i\omega_n \end{bmatrix} \ , \tag{6}$$

with the screened electron-ion interaction

$$g_\alpha \begin{bmatrix} l \\ \kappa , \mathbf{r}, i\omega_n \end{bmatrix} = \int d\mathbf{r}'\, \epsilon^{-1}(\mathbf{r}\mathbf{r}', i\omega_n) \frac{\partial V(\mathbf{r}')}{\partial x_\alpha \begin{bmatrix} l \\ \kappa \end{bmatrix}} \ . \tag{7}$$

Equation (6) shows that both vertices should be fully screened in calculations of $\delta\Phi$.

It is obvious that only the properties of the electronic spectrum near the Fermi surface will enter in the change $\delta\Pi$. It is then convenient to introduce a quasiparticle description and to write G in $\mathbf{k}\omega_n$ space as[22]

$$G^{-1}(\mathbf{k}, i\epsilon_n) = Z_c \tilde{G}^{-1}(\mathbf{k}, i\epsilon_n) \ , \tag{8}$$

$$\tilde{G}^{-1}(\mathbf{k}, i\epsilon_n) = \tilde{Z}_{\mathrm{ph}}(\mathbf{k}, i\epsilon_n) i\epsilon_n - \tilde{\varepsilon}(\mathbf{k})\tau_3 - \tilde{\Phi}(\mathbf{k}, i\epsilon_n)\tau_1 \ , \tag{9}$$

with

$$Z_c = 1 - \left. \frac{\partial \Sigma_c(\mathbf{k}, i\epsilon_n)}{\partial(i\epsilon_n)} \right|_{i\epsilon_n \to 0,\ \mathbf{k} \text{ on FS}} \ , \tag{10}$$

$$\tilde{\varepsilon}(\mathbf{k}) = \epsilon(\mathbf{k})/Z_c \ , \tag{11}$$

$$1 - \tilde{Z}_{\mathrm{ph}} = \frac{1 - Z_{\mathrm{ph}}}{Z_c} \ , \tag{12}$$

$$\tilde{\Phi}=\Phi/Z_c \ . \tag{13}$$

Σ_c is the Coulomb part of the normal electronic self-energy, and FS stands for Fermi surface. In principle, Z_c may still depend on the direction of $\mathbf{k}$. However, this is not the case if one assumes cylindrical symmetry for the band structure near the Fermi surface, which we will do in the following. τ_1 and τ_3 are Pauli matrices. $Z_{\rm ph}$ and Φ are Eliashberg functions due to the lowest-order self-energy diagram of the electron-phonon interaction. Strictly speaking, there are additional contributions to $\tilde{\varepsilon}$ due to the electron-electron and the electron-phonon interactions [see Eqs. (59) and (60) in Ref. 22], which we will neglect in the following. In view of our application to high-T_c oxides, the main assumption underlying the above equations is the neglect of the frequency dependence of Z_c because the derivative of the right-hand side in Eq. (10) is taken for $i\epsilon_n \to 0$. Such an approximation is justified if the interesting energy range for quasiparticles (which in our case is determined by phonon energies and the temperature) is much smaller than the Fermi energy ε_F. In high-T_c oxides typical values are $\omega_{\rm ph}\sim 0.05-0.1$ eV and $\varepsilon_F\sim 0.1-0.3$ eV, so that the above approximation may be problematic from a quantitative point of view.

Within a one-band model, Eq. (3) can be rewritten in $\mathbf{k}$ space as

$$\Pi(\mathbf{k},i\omega_n)=\frac{T}{Z_c}\sum_{\mathbf{k}'\epsilon_{n'}} \mathrm{Tr}\left[\tau_3\tilde{G}(\mathbf{k}'+\mathbf{k},i\epsilon_{n'}+i\omega_n)\frac{\Gamma'(\mathbf{k}'+\mathbf{k},\mathbf{k}',i\epsilon_{n'}+i\omega_n,i\epsilon_{n'})}{Z_c}\tilde{G}(\mathbf{k}',i\epsilon_{n'})\right] . \tag{14}$$

Approximating Γ' by its normal-state value [similarly as Σ_c has been approximated by its normal-state value in Eq. (10)], the ratio Γ'/Z_c approaches $-\tau_3$ in the limit $i\omega_n$, $\mathbf{k}\to 0$, which can easily be obtained from the Ward identity Eq. (8-93b) in Ref. 21 (our Γ' is identical with Γ_0 of Ref. 21).

In order to calculate Π, it is not unreasonable to approximate Γ'/Z_c by $-\tau_3$ also for finite values of $\mathbf{k}$ and ω_n. Coulomb correlations then enter Π only via the explicit factor Z_c and the appearance of quasiparticle energies $\tilde{\varepsilon}$ in $\tilde{G}$ instead of the bare ones. The renormalized functions $\tilde{Z}_{\rm ph}$ and $\tilde{\Phi}$ in $\tilde{G}$ satisfy the usual Eliashberg equations [see Eq. (61) in Ref. 22]. Inserting the explicit expression Eq. (8) for $\tilde{G}$, we obtain

$$\Pi(\mathbf{k},i\omega_n)=\frac{2T}{Z_c}\sum_{\mathbf{k}'\epsilon_{n'}}\frac{-\tilde{Z}_{\rm ph}(i\omega_n+i\epsilon_{n'})\tilde{Z}_{\rm ph}(i\epsilon_{n'})(\omega_n+\epsilon_{n'})\epsilon_{n'}+\tilde{\varepsilon}(\mathbf{k}+\mathbf{k}')\epsilon(\mathbf{k}')-\tilde{\Phi}(i\omega_n+i\epsilon_{n'})\tilde{\Phi}(i\epsilon_{n'})}{[\tilde{Z}^2_{\rm ph}(i\omega_n+i\epsilon_{n'})(\omega_n+\epsilon_{n'})^2+E^2(\mathbf{k}+\mathbf{k}',i\omega_n+i\epsilon_{n'})][\tilde{Z}^2_{\rm ph}(i\epsilon_{n'})\epsilon^2_{n'}+E^2(\mathbf{k}',i\epsilon_{n'})]} , \tag{15}$$

with

$$E^2(\mathbf{k},i\epsilon_n)=\tilde{\varepsilon}^2(\mathbf{k})+\tilde{\Phi}^2(i\epsilon_n) \ . \tag{16}$$

As usual, we have put the $\mathbf{k}$ vector in $\tilde{Z}$ and $\tilde{\Phi}$ right on the Fermi surface. Assuming cylindrical symmetry for electron and phonon bands, $\tilde{Z}$ and $\tilde{\Phi}$ are independent of the direction of $\mathbf{k}$ so that the argument $\mathbf{k}$ can be dropped. We want to carry out analytically the sum over $\mathbf{k}'$. Because of the assumed cylindrical symmetry, the sum over k'_z is trivial. Choosing the length a of the primitive square in the CuO_2 plane and the energy $\hbar^2/2ma^2$ (m is the bare band-structure mass) as units for length and energy, respectively, we obtain

$$\Pi(\mathbf{k},i\omega_n)=\frac{2TN(0)}{Z_c}\sum_{\epsilon_{n'}}\int\frac{d^2k'}{\pi}\frac{X+\tilde{\varepsilon}(\mathbf{k}+\mathbf{k}')\tilde{\varepsilon}(\mathbf{k}')}{[Y_1+\tilde{\varepsilon}^2(\mathbf{k}')][Y_2+\tilde{\varepsilon}^2(\mathbf{k}+\mathbf{k}')]} , \tag{17}$$

with the abbreviations

$$X=-\tilde{Z}_{\rm ph}(i\omega_n+i\epsilon_{n'})\tilde{Z}_{\rm ph}(i\epsilon_{n'})(\omega_n+\epsilon_{n'})\epsilon_{n'}-\tilde{\Phi}(i\omega_n+i\epsilon_{n'})\tilde{\Phi}(i\epsilon_{n'}) , \tag{18}$$

$$Y_1=\tilde{Z}^2_{\rm ph}(i\epsilon_{n'})\epsilon^2_{n'}+\tilde{\Phi}^2(i\epsilon_{n'}) , \tag{19}$$

$$Y_2=\tilde{Z}^2_{\rm ph}(i\omega_n+i\epsilon_{n'})(\omega_n+\epsilon_{n'})^2+\tilde{\Phi}^2(i\omega_n+i\epsilon_{n'}) \ . \tag{20}$$

$N(0)$ is the density of bare electronic states at the Fermi surface and equal to $1/4\pi$ in our units. $\tilde{\varepsilon}(\mathbf{k})$ is given by

$$\tilde{\varepsilon}(\mathbf{k})=\frac{\mathbf{k}^2}{Z_c}-\tilde{\mu} , \tag{21}$$

where $\mathbf{k}$ represents always a two-dimensional vector and $\tilde{\mu}$ is the chemical potential for quasiparticles. Decomposing the fraction under the integral sign in Eq. (17) into partial fractions, one finds after some algebra that

$$\Pi(\mathbf{k},i\omega_n)=-\frac{T}{2}N(0)\sum_{\epsilon_{n'}}\sum_{j,l=1}\left[\frac{(-1)^{j+l}X}{\sqrt{Y_1Y_2}}-1\right]I(\mathbf{k}/\sqrt{Z_c},\alpha_j,\beta_l) , \tag{22}$$

with

$$\alpha_j=\tilde{\mu}-(-1)^j i\sqrt{Y_1}\ , \tag{23}$$

$$\beta_l=\tilde{\mu}-(-1)^l i\sqrt{Y_2}-\mathbf{k}^2\ , \tag{24}$$

$$I(\mathbf{k},\alpha,\beta)=\int\frac{d^2k'}{\pi}\frac{1}{(\mathbf{k}'^2-\alpha)(\mathbf{k}'^2+2\mathbf{k}'\cdot\mathbf{k}-\beta)}\ . \tag{25}$$

In the Appendix it is shown that

$$I(\mathbf{k},\alpha,\beta)=\frac{1}{[(\alpha-\beta)^2-4\alpha\mathbf{k}^2]^{1/2}}\left[-\ln(y_1-\mathbf{k}^2)+\ln(y_1)+\ln(\mathbf{k}^2-y_2)-\ln(-y_2)\right.$$
$$+2\pi i\Theta\left(\mu+\mathbf{k}^2\frac{\bar{\alpha}\bar{\beta}}{(\bar{\alpha}-\bar{\beta})^2}\right)\{[\Theta(-\bar{\beta})+\Theta(-\bar{\alpha})]\Theta(\bar{\alpha}+\bar{\beta})$$
$$\left.-[\Theta(\bar{\beta})+\Theta(\bar{\alpha})]\Theta(-\bar{\alpha}-\bar{\beta})\}\right]\ , \tag{26}$$

with

$$y_{1,2}=\frac{\alpha-\beta\pm[(\alpha-\beta)^2-4\alpha\mathbf{k}^2]^{1/2}}{2}\ , \tag{27}$$

$$\alpha=\tilde{\mu}-i\bar{\alpha}\ , \tag{28}$$

$$\beta=\tilde{\mu}-i\bar{\beta}-\mathbf{k}^2\ , \tag{29}$$

with real $\bar{\alpha},\bar{\beta}$. ln denotes the principal branch of the complex logarithmic function.

Equation (22) for $\Pi(\mathbf{k},i\omega_n)$ approaches a nonzero value in the limit $\omega_n\to\infty$. This wrong asymptotic behavior is due to the fact that we have first carried out the $\mathbf{k}$ sum without any cutoff and then the frequency sum. The correct procedure is to do first the frequency sum and then the $\mathbf{k}$ sum (or, equivalently, first the $\mathbf{k}$ sum with a finite cutoff, then the frequency sum, and finally sending the cutoff to infinity). The resulting Π is still given by Eq. (22), however, with the asymptotic value for $\omega_n\to\infty$ subtracted off. In the following we are interested only in the change of Π due to superconductivity, i.e., in $\delta\Pi=\Pi-\Pi_N$, where Π_N denotes the normal part of Π. In this case the artificial constant at infinity is subtracted out automatically and thus does not play any role. From Eq. (22) it follows that $\Pi(\mathbf{k},0)=0$ for any $\mathbf{k}$ and that $\Pi_N(\mathbf{k},0)=0$ for $\mathbf{k}\neq 0$. Consequently, $\delta\Pi(\mathbf{k},0)=0$ for $\mathbf{k}\neq 0$, whereas $\delta\Pi(0,0)\neq 0$ as discussed in Refs. 11 and 12. After the analytic continuation to real frequencies, this implies that $\lim_{\omega\to 0}\delta\Pi(\mathbf{k},\omega)=0$ for $\mathbf{k}\neq 0$, whereas $\lim_{\omega\to 0}\delta\Pi(0,\omega)\neq 0$. The underlying discontinuity is caused by the normal contribution.

The Z_c dependence of Π can be read off from the explicit expression Eq. (22) and is given by

$$\Pi(\mathbf{k},i\omega_n)=\Pi^{(0)}\left(\frac{\mathbf{k}}{\sqrt{Z_c}},i\omega_n\right)\ , \tag{30}$$

where $\Pi^{(0)}$ is the expression for Π without Coulomb correlations, i.e., with $Z_c=1$. Equation (30) shows that the Coulomb enhancement factor Z_c does not enter Π as a prefactor. This means that the density of states in Π is that of the one-particle band structure. Coulomb correlations should therefore not enter substantially the calculations of $\mathbf{k}=0$ phonons, which may be one reason for the success of such calculations.[9] The momentum dependence of Π scales with $Z_c^{-1/2}$. In view of Eq. (30) it is also sufficient to calculate only $\Pi^{(0)}(\mathbf{k},i\omega_n)$. $\Pi^{(0)}$ depends on $\tilde{\mu}$, $\tilde{Z}_{\rm ph}(i\epsilon_n)$, and $\tilde{\Phi}(i\epsilon_n)$ as well as on T and $\mathbf{k}$. For $\mathbf{k}=0$, $\Pi^{(0)}$ is independent of $\tilde{\mu}$, which reflects the fact that no cutoff was used for the $\mathbf{k}'$ integration. For a finite $\mathbf{k}$ $\Pi^{(0)}$ depends on $\tilde{\mu}$: For instance, one of the Θ functions in Eq. (26) contains $\tilde{\mu}$ and may become zero if $|\mathbf{k}|\geq 4\sqrt{\tilde{\mu}}$.

Performing the analytic continuation with Padé approximants,[23] we have calculated $\delta\Pi^{(0)}(\mathbf{k},\omega)=\Pi^{(0)}(\mathbf{k},\omega)-\Pi_N^{(0)}(\mathbf{k}\omega)$, where $\Pi_N^{(0)}$ denotes the normal part of $\Pi^{(0)}$. For the strong-coupling calculations, we used the $\alpha^2F(\omega)$ function of Ref. 18 calculated, however, in a slightly modified way: Local-field effects in the dielectric function of CuO_2 layers in the direction were included (which did not change the results of Ref. 18 substantially); in view of recent photoemission data,[24] we used now the value $2k_F=1$ Å^{-1} instead of $2k_F=0.7$ Å^{-1} as in Ref. 18. As a result, the long-range forces are more effectively screened, leading to a reduction of the $\alpha^2F(\omega)$ values by roughly a factor of 0.65. The corresponding λ is now ~ 3.2 instead of ~ 4.8 as in Ref. 18 [the quoted value for λ corresponding to the calculated $\alpha^2F(\omega)$ values in Ref. 18 was too small by a factor 2 by mistake]. Using $\mu^*=0.15$, T_c becomes 95 K and the ratio $2\Delta(T=0)/T_c=5.6$. As pointed out in Ref. 18, the calculated absolute values for $\alpha^2F(\omega)$ are subject to a considerable uncertainty. For instance, Fermi-liquid corrections imply that the density of states prefactor in $\alpha^2F(\omega)$ is $N(0)Z_c$ if one accepts that the cancellation between the Coulomb vertex and Z_c takes place for all relevant momenta and frequencies and not just in the hydrodynamic limit. Our chosen value $Z_c=3.5$ is based on photoemission data in $Bi_2Sr_2CaCu_2O_8$ (Ref. 25) and seems to be rather approximate. Also, the details of the band structure and geometry of the Fermi surface are not taken into account realistically in our tight-binding calculation with only nearest-neighbor interactions. For instance, our Fermi surface is centered around Γ and not around S as it should be according to LDA calculations and experiments.[24] On the other hand, the results presented below and in Sec. III do not depend sensitively on details of the input. This follows for instance from the fact that a

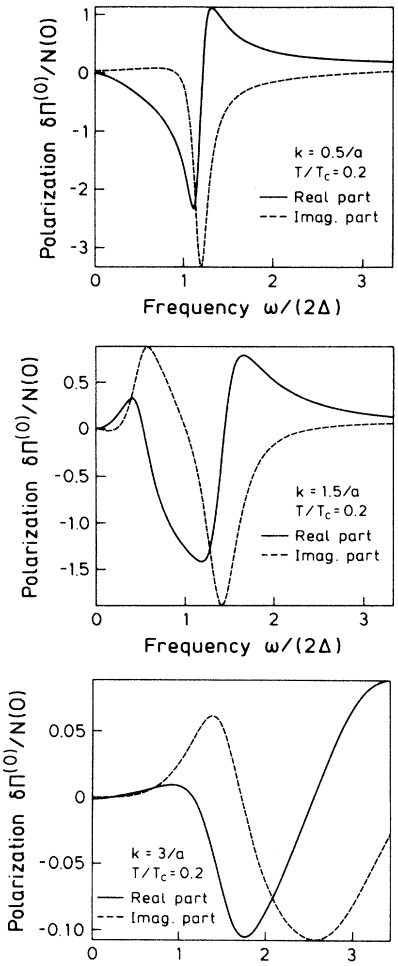

FIG. 1. Superconductivity-induced change in the real (solid line) and imaginary (dashed line) part of the polarization for $k=0.5/a$ (upper diagram), $k=1.5/a$ (middle diagram), and $k=3/a$ (lower diagram), $T/T_c=0.2$, and strong-coupling theory.

weak-coupling BCS calculation gives qualitatively and also semiquantitatively the same results as the strong-coupling calculation.

Figure 1 shows the results of strong-coupling calculations for the real (solid lines) and imaginary (broken lines) parts of $\delta\Pi^{(0)}(\mathbf{k}\omega)/N(0)$ as function of the reduced frequency $\omega/(2\Delta)$, where 2Δ is the gap at low temperatures. A general feature is that the imaginary part is positive for small frequencies due to the subtracted normal part and negative at higher frequencies due to the dominance of the superconducting part. The two curves for $k=0.5/a$ (upper diagram in Fig. 1) are similar to those for $k=0$, (see Figs. 3 and 4 of Ref. 12). There are a few minor changes: (i) The real part approaches 0 for $\omega\rightarrow 0$ for any $k\neq 0$ in contrast to the finite negative value $-2/(1+\lambda)$ at $k=0$ in agreement with the arguments given above. (ii) The imaginary part is positive and nonzero for $\omega<2\Delta$ due to the normal part. The corresponding reduction of the width of phonons below the gap due to superconductivity has been discussed and also measured for conventional superconductors.[26] (iii) The absolute values of $\delta\Pi^{(0)}$ are reduced by about a factor 2 going from $k=0$ to $0.5/a$. This reduction can easily be understood: The electron-hole transitions are oblique for a finite $\mathbf{k}$. Consequently, part of these transitions probe regions away from the Fermi surface and thus are hardly affected by the opening of the gap.

The middle diagram in Fig. 1 shows results for $k=1.5/a$, i.e., for a momentum in the middle of the Brillouin zone. The structures below 2Δ due to the normal part are clearly visible, whereas there is no major change above 2Δ. The absolute values, however, have decreased by another factor of 2 compared to the case $k=0.5/a$. The lower diagram in Fig. 1 shows results for $k=3/a$, which are substantially larger than $2k_F$. The electron-hole transitions probe now mainly regions in $\mathbf{k}$ space far away from the Fermi surface. As a result, the absolute values have decreased by more than a factor of 10 compared with $k=1.5/a$. Furthermore, the transition to the superconductivity-dominated part (negative imaginary part, positive real part) is shifted to higher frequencies.

The diagrams in Fig. 1 suggest that it might be not easy (but also not impossible) to observe superconductivity-induced changes in phonons with large momenta. Taking the results of the model calculations of Ref. 18 for granted, that the average electron-phonon coupling constant does not decrease with increasing momentum transfer, the middle diagram in Fig. 1, for instance, suggests that the maximal phonon softening in the middle of the Brillouin zone should be roughly 5 times smaller than at $k=0$, i.e., of the order of a few wave numbers. For frequencies much larger or much smaller than the gap 2Δ or for momentum transfers of about $2k_F$ or larger, the predicted effects are very small and probably undetectable in conventional neutron-scattering experiments.

III. SUPERCONDUCTIVITY-INDUCED CHANGES IN STATIC LATTICE PROPERTIES

In Sec. II we discussed dynamic effects where the superconductivity-induced self-energy of phonons is probed at one definite frequency. Static experiments, on the other hand, correspond to equal-time correlation functions and thus involve sums or integrations over the frequency in the self-energy. In the following we will consider the kinetic energy and Debye-Waller factor of one single atom in the crystal. Such calculations are interesting for two reasons: (i) Both quantities have recently been measured, and large effects due to superconductivity have been found.[27–29] (ii) They probe the electron-phonon coupling mainly at large momentum transfers and for all phonon branches similarly as superconductivity does.

The kinetic energy of an atom $\binom{l}{\kappa}$ in the direction α can be expressed as

$$T_\alpha(\kappa)=M_\kappa\left\langle\left[\dot{u}_\alpha\begin{bmatrix}l\\ \kappa\end{bmatrix}\right]^2\right\rangle$$
$$=\sum_{\mathbf{k},j}\frac{1}{2N\omega\begin{bmatrix}\mathbf{k}\\ j\end{bmatrix}}\left|e_\alpha\begin{bmatrix}\kappa\,|\,\mathbf{k}\\ j\end{bmatrix}\right|^2\left\langle\dot{A}\begin{bmatrix}\mathbf{k}\\ j\end{bmatrix}\dot{A}\begin{bmatrix}-\mathbf{k}\\ j\end{bmatrix}\right\rangle. \quad (31)$$

$e_\alpha(\kappa|{}^{\mathbf{k}}_{j})$ is the normalized eigenvector of the phonon $({}^{\mathbf{k}}_{j})$ with frequency $\omega({}^{\mathbf{k}}_{j})$ in the normal state, and we put $\hbar=1$. $A({}^{\mathbf{k}}_{j})$ is equal to $a^\dagger_{\mathbf{k}j}+a_{-\mathbf{k}j}$, where $a^\dagger_{\mathbf{k}j}$ ($a_{\mathbf{k}j}$) is the creation (destruction) operator of the phonon $({}^{\mathbf{k}}_{j})$. $\langle\ \rangle$ denotes a thermal average. Using the thermodynamic Green's function $D_{jj}(\mathbf{k}\omega_n)$, we have

$$\left\langle \dot{A}\begin{bmatrix}\mathbf{k}\\ j\end{bmatrix}\dot{A}\begin{bmatrix}-\mathbf{k}\\ j\end{bmatrix}\right\rangle = T\sum_n \omega_n^2 D_{jj}(\mathbf{k},i\omega_n)\ . \tag{32}$$

The superconductivity-induced change in the kinetic energy then becomes

$$\delta T_\alpha(\kappa)=\frac{2}{N}\sum_{k,j}\omega\begin{bmatrix}\mathbf{k}\\ j\end{bmatrix}\left|e_\alpha\begin{bmatrix}\kappa\,|\,\mathbf{k}\\ j\end{bmatrix}\right|^2 T \times\sum_n \frac{\omega_n^2}{\left[\omega_n^2+\omega^2\begin{bmatrix}\mathbf{k}\\ j\end{bmatrix}\right]^2}\delta\Sigma_j(\mathbf{k},i\omega_n)\ . \tag{33}$$

$\delta\Sigma_j(\mathbf{k},i\omega_n)$ is the superconductivity-induced change in the self-energy of the phonon $({}^{\mathbf{k}}_{j})$. It is equal to $\delta\Phi$ of Eq. (6), written in the basis of normal coordinates and divided by $2\omega({}^{\mathbf{k}}_{j})$. In obtaining Eq. (33) we have linearized $\delta T_\alpha(\kappa)$ with respect to $\delta\Sigma_j$. This is justified because in the screened ionic model the superconductivity-induced frequency shift of a phonon is always much smaller than its frequency in the normal state.

We have evaluated numerically Eq. (33) using the results of the screened ionic model discussed in Sec. II as well as Eqs. (22) and (26) for $\Pi^{(0)}(\mathbf{k},i\omega_n)$. The two curves in Fig. 2 show the change in the kinetic energy $\delta T_\alpha(\kappa)$ for $\alpha=x$ and $\kappa=$Cu(2) as function of temperature. The solid and broken lines have been calculated with the strong-coupling and BCS expressions, respectively, for $\Pi^{(0)}(\mathbf{k},i\omega_n)$. In both cases $\delta T_\alpha(\kappa)$ is negative below T_c. This lowering should not be confused with the superconductivity-induced softening of phonons.[12] In the latter case the self-energy due to superconductivity is probed right at the phonon frequency leading to large softenings of a phonon just below the gap, smaller ones well below the gap, and stiffenings for a phonon above the gap. In contrast to that, static quantities such as $\delta T_\alpha(\kappa)$ are related to sums over all frequencies. We find that all phonons contribute negatively to $\delta T_\alpha(\kappa)$ and that these contributions decrease with increasing phonon frequencies and with increasing momentum. The curves in Fig. 2 show that $\delta T_\alpha(\kappa)$ decreases rapidly just below T_c and then saturates for $T/T_c\leq\frac{2}{3}$. In the strong-coupling calculation, the gap is about 60% larger than in the BCS case, which makes $\delta T_\alpha(\kappa)$ larger. On the other hand, the strong-coupling gap is a function of frequency and decreases with increasing frequency, which will diminish $|\delta T_\alpha|$. A comparison of the two curves in Fig. 2 indicates that the second effect dominates, leading to an overall reduction of the strong-coupling values by about a factor of 2 compared to the BCS values. Calculations for δT_z[Cu(2)] yield similar curves as in Fig. 2; in particular, the magnitude of the drop in the kinetic energy is not substantially smaller than for $\alpha=x$. The calculated temperature dependence of δT_x[Cu(2)] is similar to that in the experiment of Ref. 27 for $Bi_2Sr_2CaCu_2O_8$. However, the absolute values severely disagree: The theory predicts a maximum drop of about one-tenth of a degree, whereas the experiment finds a drop of at least 20 K. Also, the large difference between δT_x and δT_z observed experimentally (δT_x does not exhibit any substantial drop experimentally) does not agree with the theoretical curves.

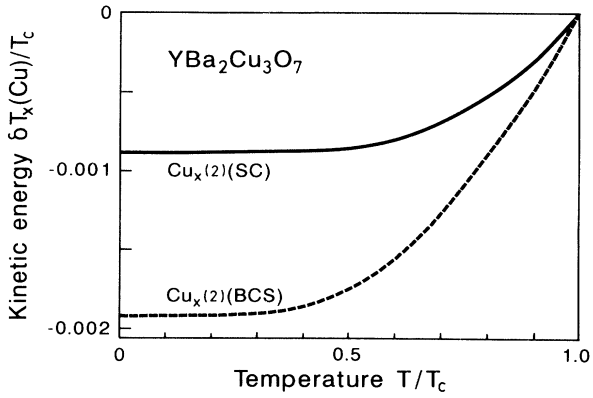

FIG. 2. Superconductivity-induced change in the kinetic energy δT_x[Cu(2)]$/T_c$ as a function of temperature T for strong-coupling (solid line) and BCS (dashed line) theory.

The following approximate analytic calculation may be helpful for an understanding of the smallness of the theoretical δT_α obtained above by numerical means. A similar calculation as in Ref. 12 yields, for $\delta\Sigma_j^{(0)}(0,i\omega_n)$,

$$\delta\Sigma_j^{(0)}(0,i\omega_n)=-8N(0)|g_j(0)|^2\left[\frac{\Delta^2}{(\omega_n^2+4\Delta^2)^{1/2}\times|\omega_n|}\right]\ln\left[\frac{(\omega_n^2/4+\Delta^2)^{1/2}+|\omega_n|/2}{\Delta}\right]\ . \tag{34}$$

We replace $\delta\Sigma_j(\mathbf{k},i\omega_n)$ in Eq. (33) by $\delta\Sigma_j^{(0)}(0,i\omega_n)/f$, where f is a suitable factor that corrects for the decrease of $\delta\Pi_j(\mathbf{k},i\omega_n)$ with increasing momentum. Inserting then Eq. (34) into Eq. (33), taking the limit $T\to0$, and neglecting the $\mathbf{k}$ dependence of the phonon branches, we obtain, after some straightforward algebraic manipulations,

$$\delta T_\alpha(\kappa)\sim\frac{-8N(0)}{\pi f\Delta}\sum_j\omega\begin{bmatrix}0\\ j\end{bmatrix}|g_j(0)|^2\left|e_\alpha\begin{bmatrix}\kappa\,|\,0\\ j\end{bmatrix}\right|^2\int_0^\infty dy\frac{\ln(\sqrt{1+y}/4+\sqrt{y}/2)}{\left[y+\omega^2\begin{bmatrix}0\\ j\end{bmatrix}/\Delta^2\right]\sqrt{4+y}}\ . \tag{35}$$

In order to proceed we replace $\omega({}^{0}_{j})$ by an average phonon energy ω_0 and put it equal to 2Δ to be able to carry out the

above integral analytically. Introducing an average branch coupling constant $\lambda_\alpha(\kappa)$ defined by

$$\lambda_\alpha(\kappa)=\frac{2N(0)}{T_c}\sum_j |g_j(0)|^2 \left|e_\alpha\left[\kappa\left|\begin{matrix}0\\ j\end{matrix}\right.\right]\right|^2 , \tag{36}$$

Eq. (35) becomes

$$\frac{\delta T_\alpha(\kappa)}{T_c}=-\frac{1}{6f}\lambda_\alpha(\kappa) . \tag{37}$$

A direct evaluation yields $\lambda_x[\mathrm{Cu}(2)]=0.072$, which is near to the average branch value $3.2/39\sim 0.08$. The value of f is about 5, yielding $\delta T_x[\mathrm{Cu}(2)]/T_c\sim 0.002$, in close agreement with the above numerical value.

A slight modification of Eqs. (31)–(33) gives for the superconductivity-induced change of the Debye-Waller factor

$$\delta\left\langle u_\alpha^2\left[\begin{matrix}l\\ \kappa\end{matrix}\right]\right\rangle=-\frac{2}{N}\sum_{\mathbf{k},j}\frac{\omega\left[\begin{matrix}\mathbf{k}\\ j\end{matrix}\right]}{M_\kappa}\left|e_\alpha\left[\kappa\left|\begin{matrix}\mathbf{k}\\ j\end{matrix}\right.\right]\right|^2 T\sum_n \frac{\delta\Sigma_j(\mathbf{k},i\omega_n)}{\left[\omega_n^2+\omega^2\left[\begin{matrix}\mathbf{k}\\ j\end{matrix}\right]\right]^2} . \tag{38}$$

Figure 3 shows the numerically evaluated left-hand side of Eq. (38) divided by the Debye-Waller factor of the harmonic lattice. In the calculation use has been made of the results of the screened ionic model. The solid and broken lines show the case $\alpha=x$, $\kappa=\mathrm{O}(2)$ in the strong- and weak-coupling cases, respectively. The dot-dashed line corresponds to $\alpha=z$, $\kappa=\mathrm{O}(2)$ and the strong-coupling case. All the curves increase below T_c and saturate only at low temperatures. The increase of the Debye-Waller factor below T_c corresponds to the decrease of the kinetic energy below T_c discussed above. The difference between the strong- and weak-coupling cases is rather small for O_x, meaning that the increase and decay of the gap with frequency of strong-coupling theory compensate each other to a large extent. Comparison of O_x and O_z shows that the change in the Debye-Waller factor for displacements vertical to the planes is only slightly reduced to that for displacements parallel to the planes. The absolute values of the relative change in the Debye-Waller factors are tiny and of the order of 0.1%.

A comparison of calculated Debye-Waller factor with experimental ones is presently not straightforward. X-ray-absorption fine-structure (XAFS) measurements do not show clear superconductivity-related changes of Debye-Waller factors for motions within the planes.[30,31] This agrees with our calculations. However, XAFS data indicate large superconductivity-related changes associated with the apex oxygen.[31] These changes are presumably connected with charge transfers between chains and planes which are not taken into account in our tight-binding model and therefore are absent in our calculations. On the other hand, the channeling data of Refs. 28 and 29 probe, in the usual interpretation, Debye-Waller factors for displacements perpendicular to the channeling direction, i.e., parallel to the planes. The observed large and T_c related changes disagree severely with our calculated curves. We consider the similar disagreement with the Cu nuclear-absorption resonance experiment,[27] mentioned above, even more serious because the interpretation seems very straightforward in this case. Both discrepancies point in the same direction: The displacements of atoms associated with the electronic rearrangement due to superconductivity are much larger than our strong-coupling theory with $\lambda\sim 3$ predicts. To come closer to the experimental values λ would have to be increased by at least one order of magnitude. The resulting huge coupling constants seem to be unacceptable. A more probable reason for the above discrepancies may lie in a breakdown of the harmonic approximation for the phonons in the normal state: A low Fermi energy together with a strong electron-phonon interaction may cause strongly anharmonic, frequency-dependent renormalizations of interatomic potentials[32] which we have neglected. It seems plausible that, for instance, a double-well potential could produce more easily large changes in Debye-Waller factors and kinetic energies in response to an electronic rearrangement than a harmonic well.

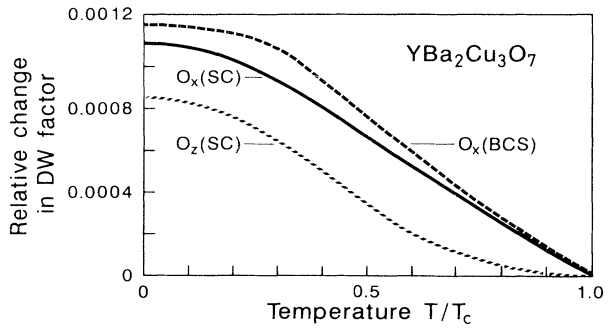

FIG. 3. Superconductivity-induced change in the Debye-Waller factor as function of the temperature for strong-coupling (solid line) and BCS (dotted) theory for displacements parallel to the planes and for strong-coupling (dotted line) theory for displacements vertical to the planes.

ACKNOWLEDGMENTS

The author acknowledges many discussions with participants (in particular G. F. Maksimov, S. Barisic, and M. Kulic) of a high-T_c workshop at the Institute for

Scientific Interchange, Torino, Italy, where part of this work has been performed. He is also grateful to A. B. Kaiser for a critical reading of the manuscript and several useful comments.

APPENDIX

The integral I defined in Eq. (25) plays a major role in the calculation of the **k**-dependent self-energy and Debye-Waller factor. We therefore give in this appendix a derivation of its explicit expression Eq. (26).

For real α,β with $\alpha<0$, $\beta<-q^2$ I is convergent and can be most easily be calculated using Feynman's technique of folding two energy denominators into one. Applying Eq. A8-1 of Ref. 33, all the appearing integrals can be carried out, and one obtains

$$I=\frac{1}{[(\alpha-\beta)^2-4\alpha k^2]^{1/2}} \times[-\ln(y_1-k^2)+\ln(y_1)+\ln(k^2-y_2)-\ln(-y_2)] , \tag{A1}$$

with

$$y_{1,2}=\frac{\alpha-\beta\pm[(\alpha-\beta)^2-4\alpha k^2]^{1/2}}{2} . \tag{A2}$$

We need the integral I for the arguments

$$\alpha=\mu-i\bar{\alpha} , \tag{A3}$$

$$\beta=\mu-i\bar{\beta}-k^2 , \tag{A4}$$

with real $\bar{\alpha},\bar{\beta}$ and $\bar{\alpha}\neq 0$, $\bar{\beta}\neq 0$. We also assume first $\bar{\alpha}\neq\bar{\beta}$. Since I is analytic for $\bar{\alpha}\neq 0$, $\bar{\beta}\neq 0$, we can define I for the special values $\bar{\alpha}=\bar{\beta}$ and $\bar{\alpha}=-\bar{\beta}$ by the limits $\bar{\alpha}\to\pm\bar{\beta}$.

Let us define linear paths by

$$\alpha(t)=-A+(\mu-i\bar{\alpha}+A)t , \tag{A5}$$

$$\beta(t)=-A-k^2+(\mu-i\bar{\beta}+A)t , \tag{A6}$$

with $A>0$ and $t\in[0,1]$. A necessary condition that the argument of the square root crosses the cut $[-\infty,0]$ of the square root is $\bar{\alpha}+\bar{\beta}=0$, which has been excluded above. The analytic continuation of the square root can thus be accomplished by using the usual principal branch of ln. Similar considerations show that the arguments y_1 and k^2-y_2 never cross the cut of the logarithm function, so that the analytic continuation of the second and third terms in parentheses in Eq. (A1) can be achieved again by using the principal branch of ln.

The analytic continuation of the first term in parentheses of Eq. (A1) needs more care. Necessary and sufficient conditions that $\bar{y}_1(t)-k^2$ crosses the negative axis are either

$$\bar{\beta}>0 , \quad \bar{\alpha}<-\bar{\beta} \tag{A7}$$

or

$$\bar{\beta}<0 , \quad \bar{\alpha}>-\bar{\beta} . \tag{A8}$$

Furthermore, the parameter value t_0 at the crossing point is given by

$$t_0=\frac{A-k^2\bar{\alpha}\bar{\beta}/(\bar{\beta}-\bar{\alpha})^2}{\mu+A} , \tag{A9}$$

which has to be in the interval [0,1]. In the case (A7) the imaginary part of $\bar{y}_1(t)-k^2$ changes near $t\sim t_0$ from positive to negative values and in the case (A6) from negative to positive values. Taken all together, the analytic continuation is achieved by the substitution

$$-\ln(y_1-k^2)\to-\ln(y_1-k^2)+2\pi i[\Theta(-\bar{\beta})\Theta(\bar{\alpha}+\bar{\beta})-\Theta(\bar{\beta})\Theta(-\bar{\alpha}-\bar{\beta})]\Theta\left[A-k^2\frac{\bar{\alpha}\bar{\beta}}{(\bar{\beta}-\bar{\alpha})^2}\right]\Theta\left[\mu+k^2\frac{\bar{\alpha}\bar{\beta}}{(\bar{\beta}-\bar{\alpha})^2}\right] . \tag{A10}$$

Analogous considerations show that the analytic continuation of the fourth term in (A1) is given by

$$-\ln(-y_2)\to-\ln(-y_2)+2\pi i[\Theta(-\bar{\alpha})\Theta(\bar{\alpha}+\bar{\beta})-\Theta(\bar{\alpha})\Theta(-\bar{\alpha}-\bar{\beta})]\Theta\left[A-k^2\frac{\bar{\alpha}\bar{\beta}}{(\bar{\beta}-\bar{\alpha})^2}\right]\Theta\left[\mu+k^2\frac{\bar{\alpha}\bar{\beta}}{(\bar{\beta}-\bar{\alpha})^2}\right] . \tag{A11}$$

Altogether, one obtains, for the integral I,

$$I=\frac{1}{[(\alpha-\beta)^2-4\alpha k^2]^{1/2}}\left[-\ln(y_1-k^2)+\ln(y_1)+\ln(k^2-y_2)-\ln(-y_2) +2\pi i\Theta\left[A-k^2\frac{\bar{\alpha}\bar{\beta}}{(\bar{\beta}-\bar{\alpha})^2}\right]\Theta\left[\mu+k^2\frac{\bar{\alpha}\bar{\beta}}{(\bar{\beta}-\bar{\alpha})^2}\right] \times\{[\Theta(-\bar{\beta})+\Theta(-\bar{\alpha})]\Theta(\bar{\alpha}+\bar{\beta})-[\Theta(\bar{\beta})+\Theta(\bar{\alpha})]\Theta(-\bar{\alpha}-\bar{\beta})\}\right] . \tag{A12}$$

The term $\sim 2\pi i$ in Eq. (A12) is nonzero only if the product $\bar{\alpha}\bar{\beta}$ is negative. This means that the function $\Theta[A-k^2\bar{\alpha}\bar{\beta}/(\bar{\beta}-\bar{\alpha})^2]$ is always 1 because of $A>0$ and thus can be dropped. Equation (A12) is then identical with Eq. (26) of Sec. II. Furthermore, it follows that

$$4\frac{\bar{\alpha}\bar{\beta}}{(\bar{\beta}-\bar{\alpha})^2} \leq 1 \ . \tag{A13}$$

This inequality implies (remember that $\mu = k_F^2$) that the function $\Theta[\mu + k^2\bar{\alpha}\bar{\beta}/(\bar{\alpha}-\bar{\beta})^2]$ is always 1 for $k \leq 2k_F$. For the special value $\bar{\alpha} = -\bar{\beta}$, I can be obtained by taking either $\bar{\alpha}\uparrow -\bar{\beta}$ or $\bar{\alpha}\downarrow -\bar{\beta}$.

[1]B. Batlogg, R. V. Cava, A. Jayaraman, R. B. van Dover, G. A. Kourouklis, S. Sunshine, D. W. Murphy, L. W. Rupp, H. S. Chen, A. White, K. J. Short, A. M. Mujsce, and E. A. Rietman, Phys. Rev. Lett. **58**, 2333 (1987).

[2]S. Martin, A. T. Fiory, R. M. Fleming, L. F. Schneemeyer, and J. V. Waszczak, Phys. Rev. B **41**, 846 (1990).

[3]J. Yu, S. Massidda, A. J. Freeman, and D. D. Koeling, Phys. Lett. A **122**, 203 (1987).

[4]P. B. Allen, W. E. Pickett, and H. Kraukauer, Phys. Rev. B **37**, 7482 (1988).

[5]W. Weber and L. F. Mattheiss, Phys. Rev. B **37**, 599 (1988).

[6]I. I. Mazin, S. N. Rashkeev, and S. Y. Savrasov, Phys. Rev. B **42**, 366 (1990).

[7]R. M. Macfarlane, H. Rosen, and H. Seki, Solid State Commun. **63**, 831 (1987).

[8]C. Thomsen and M. Cardona, in *Physical Properties of High-Temperature Superconductors I,* edited by D. M. Ginsberg (World Scientific, Singapore, 1989), Chap. 8.

[9]C. Thomsen, M. Cardona, B. Friedl, I. I. Mazin, C. O. Rodriguez, and O. K. Andersen, Solid State Commun. **75**, 219 (1990).

[10]B. Friedl, C. Thomsen, and M. Cardona, Phys. Rev. Lett. **65**, 915 (1990).

[11]R. Zeyher and G. Zwicknagl, Solid State Commun. **66**, 617 (1988).

[12]R. Zeyher and G. Zwicknagl, Z. Phys. B **78**, 175 (1990).

[13]R. E. Cohen, W. E. Pickett, and H. Kraukauer, Phys. Rev. Lett. **64**, 2575 (1990).

[14]C. O. Rodriguez, A. I. Liechtenstein, I. I. Mazin, O. Jepsen, O. K. Andersen, and M. Methfessel, Phys. Rev. B **42**, 2692 (1990).

[15]S. J. Hagen, Z. Z. Wang, and N. P. Ong, Phys. Rev. B **40**, 9389 (1989).

[16]C. Uher, J. Supercond. **3**, 337 (1990).

[17]L. Tewordt and Th. Wölkhausen, Solid State Commun. **70**, 839 (1989).

[18]R. Zeyher, Z. Phys. B **80**, 187 (1990).

[19]S. L. Chaplot, Phys. Rev. B **37**, 7435 (1988).

[20]L. J. Sham, Phys. Rev. **188**, 1431 (1969).

[21]J. R. Schrieffer, *Theory of Superconductors* (Benjamin, Reading, MA, 1986).

[22]D. J. Scalapino, in *Superconductivity,* edited by R. D. Parks (Dekker, New York, 1969), Vol. 1, Chap. 10.

[23]H. J. Vidberg, and J. W. Serene, J. Low Temp. Phys. **29**, 179 (1977).

[24]J. C. Campuzano, G. Jennings, M. Faiz, L. Beaulaigue, B. W. Veal, J. Z. Liu, A. P. Paulikas, K. Vandervoort, H. Claus, R. S. List, A. J. Arko, and R. J. Bartlett, Phys. Rev. Lett. **64**, 2308 (1990).

[25]G. Mante, R. Claessen, T. Buslaps, S Harm, R. Manzke, M. Skibowski, and J. Fink, Z. Phys. B **80**, 181 (1990).

[26]S. M. Shapiro, G. Shirane, and J. D. Axe, Phys. Rev. B **12**, 4899 (1975).

[27]H. A. Mook, M. Mostoller, J. A. Harvey, N. W. Hill, B. C. Chakoumakos, and B. C. Sales, Phys. Rev. Lett. **65**, 2712 (1990).

[28]R. P. Sharma, L. E. Rehn, P. M. Baldo, and J. Z. Liu, Phys. Rev. Lett. **62**, 2869 (1989).

[29]T. Haga, K. Yamaya, Y. Abe, Y. Tayima, and Y. Hidaka, Phys. Rev. B **41**, 826 (1990).

[30]H. Maeda, N. Bamba, A. Koizumi, Y. Yoshikawa, T. Ishii, H. Maruyama, M. Hida, Y. Kuroda, H. Yamazaki, and T. Morimoto, J. Phys. Soc. Jpn. **56**, 3413 (1987).

[31]S. D. Conradson, I. D. Raistrick, and A. Bishop, Science **248**, 1394 (1990).

[32]C. C. Yu and P. W. Anderson, Phys. Rev. B **29**, 6165 (1984).

[33]D. J. Amit, *Field Theory, the Renormalization Group, and Critical Phenomena* (World Scientific, Singapore, 1989).